Available on CMS information server

CMS NOTE 1998/020

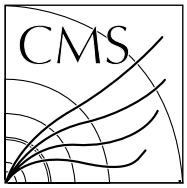

The Compact Muon Solenoid Experiment

CMS Note

Mailing address: CMS CERN, CH-1211 GENEVA 23, Switzerland

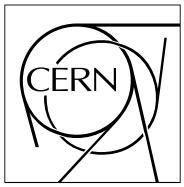

16 March 1998

Impact of Muon Trigger coverage on physics

R. Kinnunen

Helsinki Institute of Physics, Helsinki, Finland

M. Bedjidian

Institut de Physique Nucléaire, Lyon, France

S. Abdullin[a)]

UHA, Mulhouse, France

D. Denegri

DAPNIA, CEN Saclay, France

I. Iashvili[b)], A. Kharchilava[b)], L. Rurua[c)]

Institute of Physics, Georgian Academy of Sciences, Tbilisi, Georgia

C. Albajar

Universidad Autonoma de Madrid, Madrid, Spain

A. Nikitenko[a)], G. Wrochna

CERN, Geneva, Switzerland

Abstract

Acceptance for selected physics channels is calculated as a function of muon trigger coverage in η.

[a)] On leave from *ITEP, Moscow, Russia*

[b)] Currently at *DESY-IfH Zeuthen, Germany*

[c)] Currently at *Institut für Hochenergiephysik, Österreichische Akademie d.Wissenschaften, Vienna, Austria*

1 Introduction

There are at least three reasons to study how the limited trigger acceptance can influence the physics reach of CMS. First, changing the pseudorapidity range $\eta^{\mu}_{\rm trig}$ (together with transverse momentum threshold $p_t^{\rm cut}$) is a tool to control the First Level Trigger (LV1) output rate. It has to be kept below the acceptable Second Level Trigger (LV2) rate.

Second, the rate of background rises dramatically with η. The muon detector is designed to cope with the expected level of background assuming a safety factor of 2-10. However, if the background is higher still, it may result in production of ghosts, fake muons, false triggers, etc. In this case reducing $\eta^{\mu}_{\rm trig}$ might improve the overall signal to background ratio (S/B) by suppressing the background more than the signal (i.e. real muons).

Third, a possible mismatch of funding and spending profiles may require the trigger acceptance to be built up gradually, according to available resources.

One can distinguish several regions in the muon trigger coverage:

$\|\eta\| < 0.8$	barrel only
$0.8 < \|\eta\| < 1.2$	barrel/endcap overlap
$1.2 < \|\eta\| < 1.6$	endcap without ME/1-4/1 chambers
$\|\eta\| < 2.1$	baseline RPC coverage
$\|\eta\| < 2.4$	full muon acceptance

These regions are indicated in Fig. 1. The η values listed in the table are the natural places where to limit the trigger acceptance, if it were necessary.

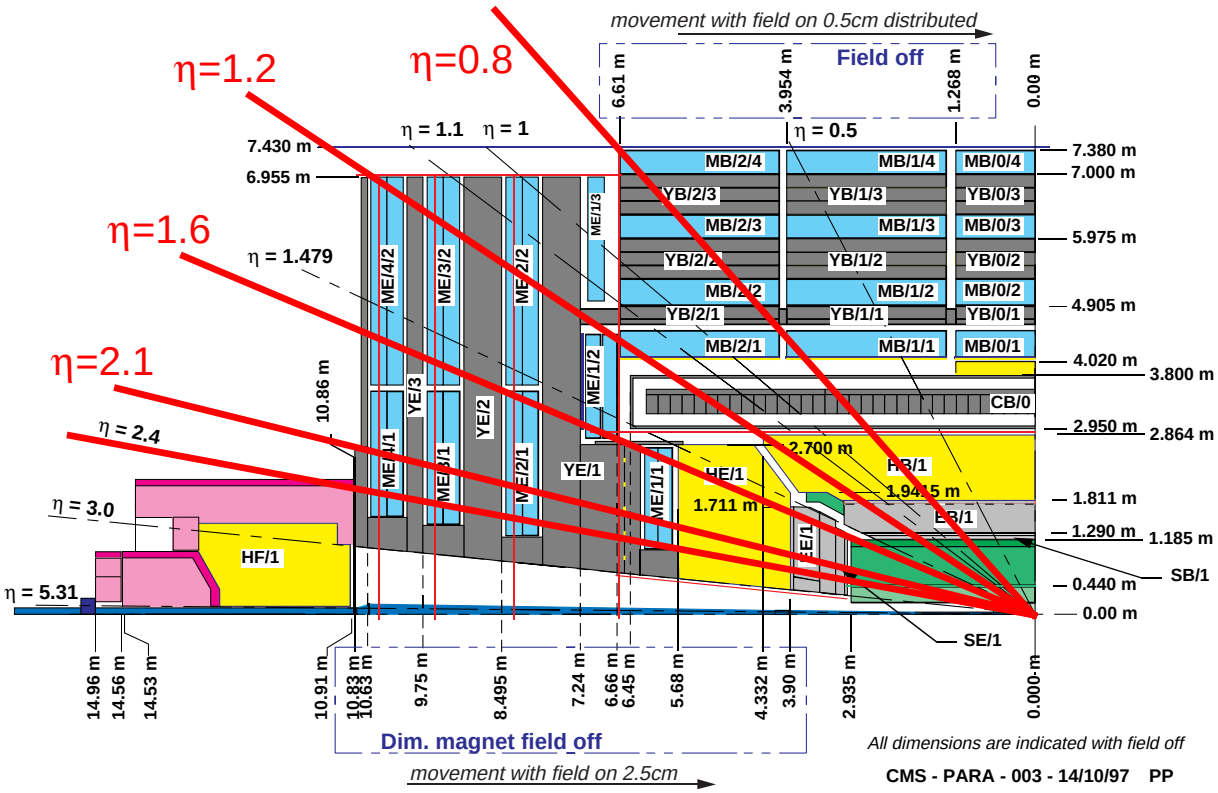

Figure 1: Muon trigger regions.

In the following sections we examine the expected performance loss as a function of muon trigger acceptance for some of the most important physics channels to be studied at CMS. The acceptance for each channel is calculated as a function of muon trigger coverage $\eta^{\mu}_{\rm trig}$ for fixed off-line measurement coverage of $\eta^{\mu}_{\rm meas}$=2.4. It is normalised to the full muon detector coverage of $\eta^{\mu}_{\rm trig}$=2.4. In some cases we also compare it to the full acceptance of ATLAS which is $\eta^{\mu}_{\rm trig}$=2.4 for the trigger and $\eta^{\mu}_{\rm meas}$=2.7 for the off-line measurement.

2 Standard Model Higgs

The leptonic (μ or e) decays of Higgs with a mass of 130 GeV were generated by PYTHIA [1]:

$$\mathrm{H} \longrightarrow \mathrm{ZZ}^* \longrightarrow 4\mu \quad (2.1)$$
$$\mathrm{H} \longrightarrow \mathrm{ZZ}^* \longrightarrow 2\mu + 2e \quad (2.2)$$

The high luminosity triggers are considered. Fig. 2 shows the relative acceptance versus $\eta^{\mu}_{\mathrm{trig}}$ coverage of muon trigger system. In all cases a logical OR of single and dimuon triggers have been applied. Channel (2.2) was simulated with the muon trigger only and the acceptance losses can be partially recovered with the electron trigger. A special case has been also considered assuming that the third muon in the event could be reconstructed up to $\eta^{\mu}_{\mathrm{meas}}$=2.7 in the off-line analysis (case in ATLAS). It is shown in Fig. 2 with the dashed line.

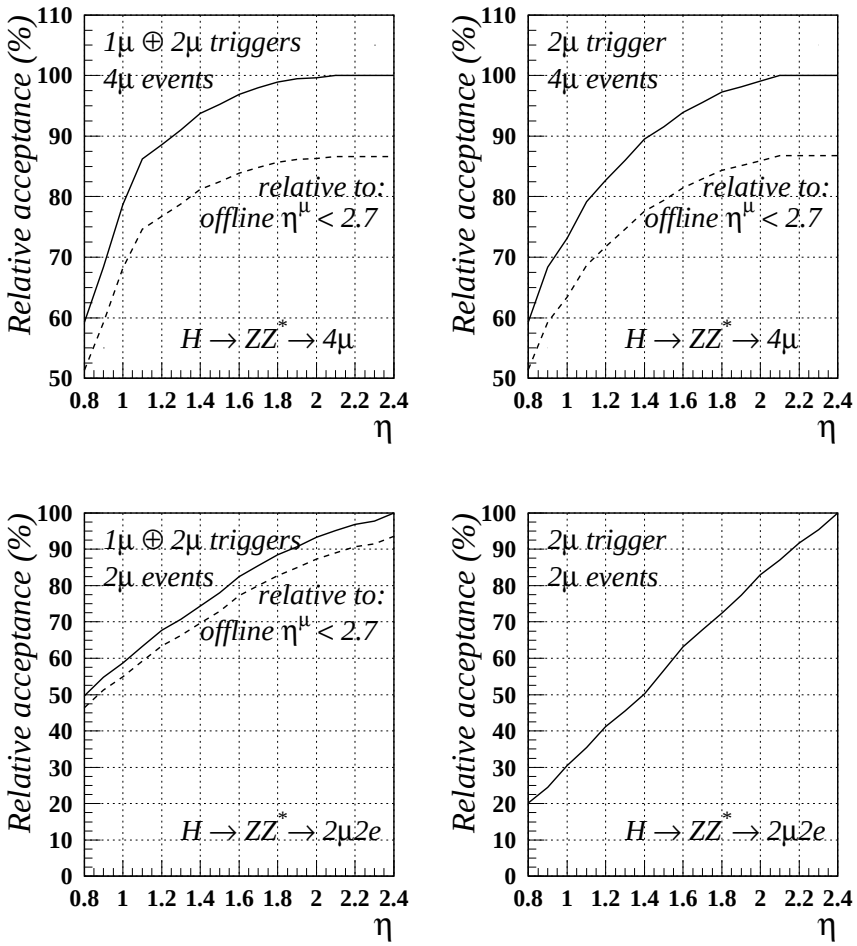

Figure 2: Relative acceptance for Higgs decays as a function of muon trigger limit $\eta^{\mu}_{\mathrm{trig}}$ for 1μ and 2μ trigger. $M_H = 130$ GeV.

In general higher is the multiplicity of final state leptons less sensitive we are to forward muon trigger acceptance losses as events can still trigger on centrally produced leptons.

3 SUSY Higgses

The channels $A, H, h \to \tau\tau$ and $H^{\pm} \to \tau\nu$, with $H^{\pm}$ produced in $t\bar{t} \to WbWH^{\pm} \to \mu_{\rm trig} + H^{\pm} + X$, will be the first channels allowing search and possibly providing first observation of the SUSY Higgs at LHC, because already at low luminosity the discovery contours cover significant areas of parameter space and approache closely the eventual LEP limits (see Fig. 3) in particular if $\sqrt{s}$ of LEP II increases to 200 GeV, gradually closing the lower m_A range. The $A, H, h \to \mu\mu$ channel has a similar coverage of parameter space as the $\tau\tau$ channel, but requires more statistics ($\sim 10^5 \mathrm{pb}^{-1}$).

The $t\bar{t} \to W_{\to \mu_{\rm trig}} b W H^{\pm}_{\to \tau\nu}$ channel is discussed in Section 5. For the $A, H, h \to \tau\tau$ study the point of $\tan\beta = 20$ and $m_A = 140$ GeV was chosen as representative of the early discovery/exclusion searches. The most promising signature for this channel is $\ell^{\pm} + \tau{-}\mathrm{jet} + E_t^{\rm miss}$, with one τ decaying leptonicaly and the second one — hadronicaly. At the First Level Trigger the coincidence of an e or μ trigger with a τ-trigger is required. The acceptance was studied for two cases

- τ-trigger × combined e and μ trigger
- τ-trigger × μ trigger alone

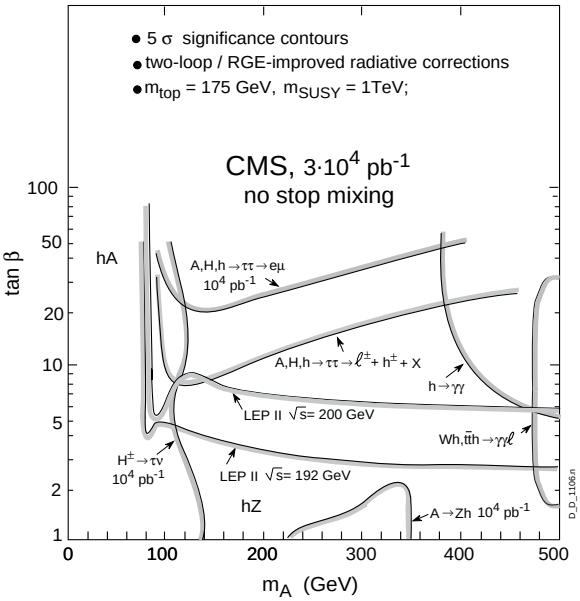

Figure 3: Regions of the MSSM parameter space $(m_A, \tan\beta)$ explorable through various Higgs channels.

Results are shown in Fig. 4. In the first case, for $p_t^{\ell} > 15$ GeV and $E_t^{\tau-\mathrm{jet}} > 40$ GeV the relative efficiency decreases linearly to 70 % if the muon trigger acceptance is reduced from $\eta^{\mu}_{\rm trig}$=2.4 to $\eta^{\mu}_{\rm trig}$=0.8. For the $\mu \times \tau$-jet trigger case with $p_t^{\mu} > 7$ GeV, the reduction is more dramatic, falling to 40 % for $\eta^{\mu}_{\rm trig}$=0.8.

The $A, H, h \to \mu\mu$ channel was studied for $\tan\beta = 30$ and $m_A = 120$ GeV. Two production mechanisms were considered separately

- $gg \to A^0 \to \mu\mu$
- $gg \to b\bar{b} + A^0 \to \mu\mu$

The relative contribution of the two channels is 2:5. The simulation was done for A^0, but similar η distributions are expected for muons from H^0 and h^0 decays. The results are shown in Fig. 5.

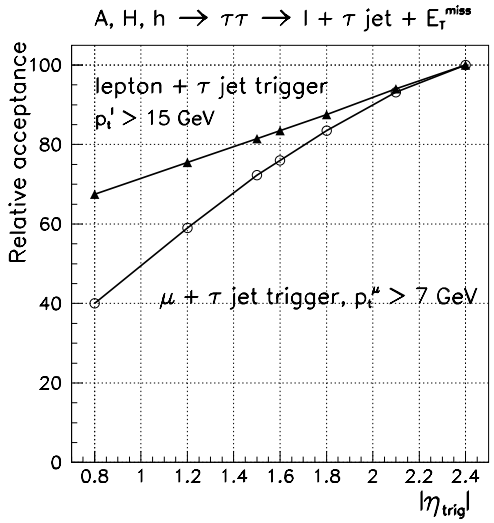

Figure 4: Relative acceptance for $A, H, h \to \tau\tau$ decays ($\tan\beta$=20, m_A=140 GeV) as a function of muon trigger limit $\eta^{\mu}_{\rm trig}$ for combined electron and muon triggers (triangles) and muon trigger alone (circles).

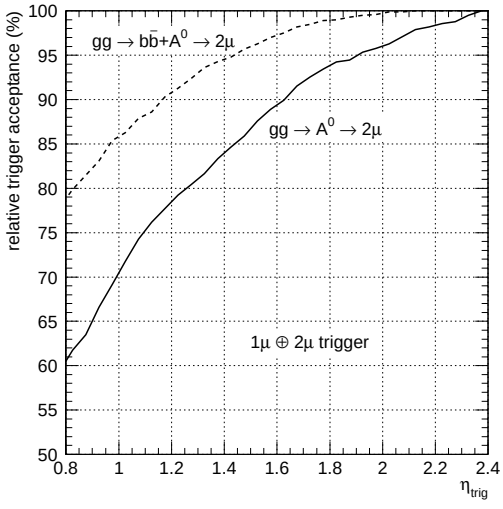

Figure 5: Relative acceptance for $A, H, h \to \mu\mu$ decays ($\tan\beta$=30, m_A=120 GeV) as a function of muon trigger acceptance limit $\eta^{\mu}_{\rm trig}$ for 1μ and 2μ triggers.

4 SUSY partners

4.1 Single lepton final states

Among the variety of leptons + jets + $E_t^{\rm miss}$ final states studied in the framework of mSUGRA-MSSM [2] the 1 lepton + jets + $E_t^{\rm miss}$ turns out to be the most promising one from the point of view of squark-gluino mass reach for CMS [3, 4]. Fig. 6 shows, for example, the mass reach for 1 fb^{-1} for different numbers of final state leptons. To see how the 1-lepton signal is affected by muon trigger acceptance reduction, we took 3 points in mSUGRA parameter space a bit above LEP and Tevatron (with 1 fb^{-1}) sparticle reaches. Three of the mSUGRA parameters were fixed: A_0=0, tanβ=2 and μ <0, and the other two parameters, m_0 and $m_{1/2}$, are varied. Table 1 gives point parameters, masses of sparticles, the average number of leptons (with $\geq$ 1) and the relative content of muons in lepton sample for $|\eta^\ell| < 2.4$. Table 2 gives the relevant decay modes and branching ratios of sparticles. It is worth mentioning that the lightest squarks, stop and sbottom, decay into top/bottom + charginos or neutralinos in a similar way in all the cases considered below.

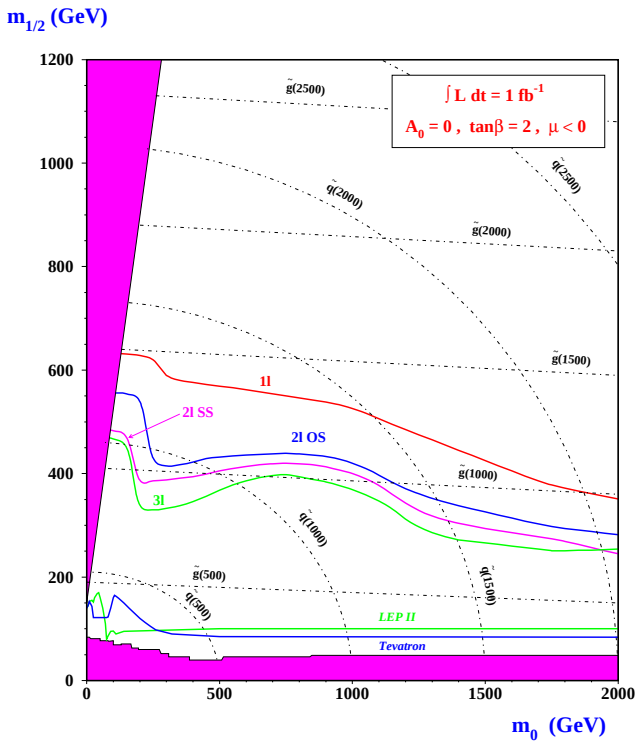

Figure 6: Domain of (m_0, $m_{1/2}$) parameter space of mSUGRA-MSSM model explorable by $\tilde{q}$ and $\tilde{g}$ searches in final states $\ell + E_t^{\rm miss}+ \geq$2 jets with 1 fb^{-1}. The reach is defined as 5σ boundaries, where $\sigma = S/\sqrt{S + B_{SM}}$.

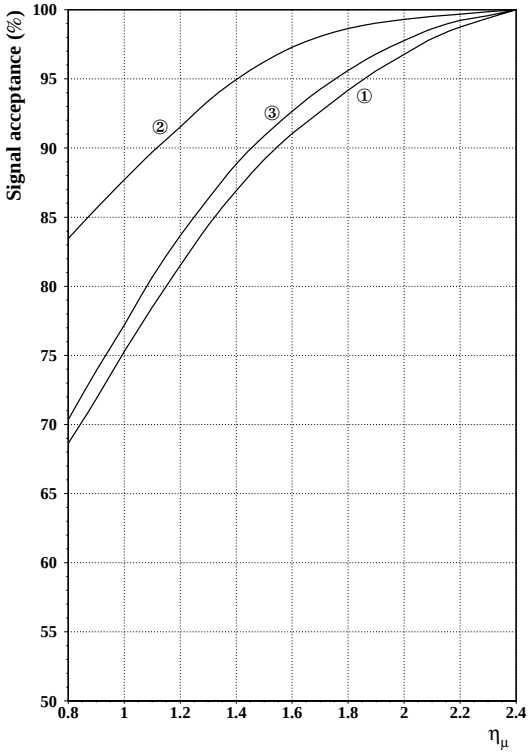

Figure 7: Relative acceptance for SUSY decays $\rightarrow \ell + E_t^{\rm miss}+ \geq$2 jets as a function of muon trigger limit $\eta^\mu_{\rm trig}$ for muon and electron trigger. Numbers in circles denote signal Points 1-3.

Table 1: Parameters of points under study.

Point	m_0 (GeV)	m_0 (GeV)	Masses of sparticles (GeV)					$\langle N_l \rangle$	N_μ/N_ℓ
			$\tilde{g}$	$\tilde{u}_L$	$\tilde{t}_1$	$\tilde{\chi}_2^0$	$\tilde{\chi}_1^0$		
1	80	180	486.6	434.9	353.8	159.1	77.7	1.61	0.71
2	200	150	422.2	412.3	325.4	135.4	65.1	1.99	0.63
3	500	150	438.3	607.9	370.0	134.5	65.0	1.73	0.74

Table 2: Main decay modes and branching ratios of sparticles.

Point	$\tilde{g}$	$\tilde{u}_L$	$\tilde{\chi}_2^0$	$\tilde{\chi}_1^\pm$
1	$\tilde{q}q$	$\tilde{\chi}_2^0\ u$ (31 %) $\tilde{\chi}_1^+\ d$ (66 %)	$\tilde{\nu}\nu$ (91 %) $\tilde{\ell}\ell$ (3 %)	$\tilde{\nu}\ell^\pm$ (64 %)
2	$\tilde{q}q$ ($\tilde{b}_{1,2}b$ 60 %)	$\tilde{\chi}_2^0\ u$ (31 %) $\tilde{\chi}_1^+\ d$ (66 %)	$\tilde{\chi}_1^0\ \ell^+\ell^-$ (32 %)	$\tilde{\chi}_1^0\ \ell^\pm\nu$ (12 %)
3	$\tilde{\chi}_{1,2}^0\ q\bar{q}$ $\tilde{\chi}_1^\pm\ q_i q_j$	$\tilde{\chi}_2^0\ u$ (14 %) $\tilde{\chi}_1^+\ d$ (29 %) $\tilde{g}\ u$ (56 %)	$\tilde{\chi}_1^0\ \ell^+\ell^-$ (8 %) $\tilde{\chi}_1^0\ b\bar{b}$ (29 %)	$\tilde{\chi}_1^0\ \ell^\pm\nu$ (20 %)

The mSUGRA signal is generated with ISAJET 7.32 [5] and processed with CMSJET 4.4 [6] fast MC to simulate CMS detector response. Each of three points is represented by a sample of 50000 events, which corresponds to 270, 170 and 400 pb^{-1} of integrated luminosity for points 1-3 respectively. We require at least 2 jets with $E_t^j >$ 40 GeV in $|\eta^j| < 3$ and $E_t^{\rm miss}>$ 100 GeV. One and only one lepton has to be detected within the acceptance, with $p_t^e > 20$ GeV in $|\eta^e| < 2.4$, and $p_t^\mu > 10$ GeV in the variable η acceptance. Muons are not required to be isolated, whilst electrons are [3].

"Point 1" differs from other points by the presence of 2-body decays of $\tilde{\chi}_2^0$ and $\tilde{\chi}_1^\pm$ into sleptons. Decays of $\tilde{\chi}_2^0$ do not play however a significant role in lepton production, the main source of leptons is the decay chain : $\tilde{q} \rightarrow \tilde{\chi}_1^\pm\ q$ $\rightarrow \tilde{\chi}_1^0\ l^\pm\ \nu\ q$.

"Point 2" is characterized by 3-body decays of $\tilde{\chi}_2^0$ and $\tilde{\chi}_1^\pm$ with a significant yield of leptons. The gluino, like in Point 1, is a bit heavier than the squarks, thus decays into them, leading to an abundant production of $\tilde{\chi}_2^0$ and $\tilde{\chi}_1^\pm$.

"Point 3" is similar to Point 2 from the point of view of $\tilde{\chi}_2^0$ and $\tilde{\chi}_1^\pm$ decays, but the gluino is now lighter than squarks (except stop), and $\tilde{g}\tilde{g}$ production dominates. The gluino has 3-body decays into $\tilde{\chi}_{1,2}^0\ q\bar{q}$ or $\tilde{\chi}_1^\pm\ qq$. The overall picture is more complicated than in Point 2, but the net result is that Point 3 has a lower yield of leptons than Point 2.

From Tables 1 and 2 one can already expect that Point 2 should be less affected by muon trigger coverage since it has the lowest relative muon content in leptonic sum and highest average number of leptons per event. Thus the second lepton can recover the event if the first one is out of acceptance. Table 3 and Fig. 6 show the dependence of the signal yield (relative to nominal $\eta^\mu_{\rm trig}$ coverage of 2.4) on muon acceptance.

Table 3: Relative signal value vs muon acceptance (% of nominal $\eta^\mu_{\rm trig}$= 2.4 coverage).

Point	$\eta^\mu_{\rm trig}$				
	2.4	2.1	1.6	1.2	0.8
1	100.0	97.7	91.1	81.5	68.6
2	100.0	99.4	97.2	91.5	83.5
3	100.0	98.4	92.7	83.7	70.3

4.2 Two lepton final states

If 'low-energy' supersymmetry (SUSY) is realised in Nature it should show up at the LHC. Once evidence for SUSY established, one of the first tasks will be to reconstruct sparticle masses and to find out the underlying model and determine model parameters. The *two same-flavour, opposite-sign leptons + $E_t^{\rm miss}$+ jets* channel, with final state electrons or muons channel was found to be good is particularly promissing for such a studies [4, 7]. The events with two same-flavour, opposite-sign leptons + $E_t^{\rm miss}$+ jets have been analyzed within the framework of the minimal Supergravity Model. The signature $\ell^+\ell^-$ + $E_t^{\rm miss}$+ jets selects the $\tilde{\chi}_2^0$ leptonic decays $\tilde{\chi}_2^0 \rightarrow \tilde{\chi}_1^0\ell^+\ell^-$, and the $\tilde{\chi}_2^0 \rightarrow \tilde{l}_{L,R}^{\pm}\ell^{\mp} \rightarrow \tilde{\chi}_1^0\ell^+\ell^-$. Within this model, $\tilde{\chi}_2^0$ has two-body decays $\tilde{\chi}_2^0 \rightarrow \tilde{l}_{L,R}^{\pm}\ell^{\mp}$ in the region $m_0 \lesssim 0.5 \cdot m_{1/2}$ of the parameter space, whereas in the region $m_0 \gtrsim 0.5 \cdot m_{1/2}$, $m_{1/2} \lesssim 200$ GeV it has three-body decays $\tilde{\chi}_2^0 \rightarrow \ell^+\ell^-\tilde{\chi}_1^0$. In both regions the dilepton mass spectrum $M_{\ell^+\ell^-}$ has a pronounced structure with a sharp edge at the kinematical endpoint $M_{\ell^+\ell^-}^{\rm max}$. The regions of the $(m_0, m_{1/2})$ parameter plane where the edge in the $M_{\ell^+\ell^-}$ spectrum is expected to be visible at different luminosities are shown in Fig. 8 [4, 7].

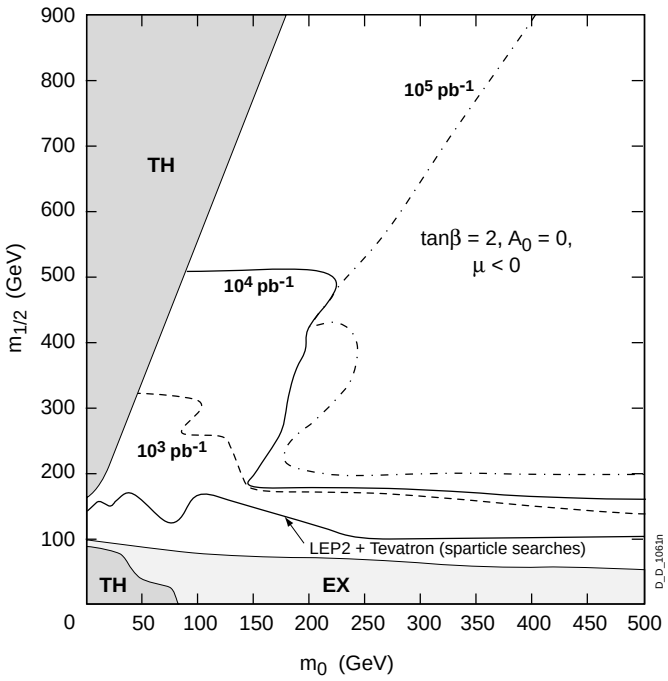

Figure 8: Domain of $(m_0, m_{1/2})$ parameter space of mSUGRA-MSSM model explorable by $\ell^+\ell^-$ + $E_t^{\rm miss}$ final states. The reach is defined as 5σ boundaries, where $\sigma = S/\sqrt{S + B_{SM}}$.

Now we discuss sensitivity of the $\ell^+\ell^-$ + $E_t^{\rm miss}$+ jets channel to muon trigger acceptance. Two cases are considered. First, a case when the electron trigger is switched on ($\eta_{\rm trig}^e$=2.4) allowing to exploit this channel, with either electrons or muons, and, second case, switching electron trigger off we are left with just $\mu^+\mu^-$ + $E_t^{\rm miss}$+ jets. The study is performed for $\int\mathcal{L} = 10^3$ pb^{-1} and $\int\mathcal{L} = 10^4$ pb^{-1}. Two representative mSUGRA points are chosen. The point m_0=105 GeV, $m_{1/2}$=181 GeV, $\tan\beta$=2, μ <0, A_0=0 is reachable already with $\int\mathcal{L} = 10^3\,pb^{-1}$ [7]. To observe an edge in the $M_{\ell^+\ell^-}$ distributions with the statistics provided by an integrated luminosity $\int\mathcal{L} = 10^3\,pb^{-1}$ it is enough to require two hard isolated leptons of $p_t^{\ell_{1,2}}$ >15 GeV with a large missing energy, $E_t^{\rm miss}$>100 GeV.

With increasing m_0 and $m_{1/2}$ cross-sections are decreasing and higher luminosity and harder cuts are needed. For a point m_0=150 GeV, $m_{1/2}$=400 GeV ($\tan\beta = 2$, $\mu < 0$, $A_0 = 0$), $10^4\,pb^{-1}$, with cuts $p_t^{\ell_{1,2}} > 20$ GeV and $E_t^{\rm miss} > 200$ GeV to suppress sufficiently the background.

Fig. 10 shows the event rate for these two points (relative to full acceptance $\eta_{\rm trig}^{\mu}$=2.4) when both electron and muon triggers are switched on. To keep the muon trigger acceptance up to at least 1.2 is important. The case when the electron trigger is switched off (Fig. 9) is much more critical. In this case a muon trigger coverage of at least $\eta_{\rm trig}^{\mu}$=1.5 is necessary for not suffering an acceptance loss in excess of 10 %. Note that this channel is not too sensitive to forward acceptance as $\ell^+\ell^-$ pairs come from chain decays of massive and centrally produced $\tilde{q}$ and $\tilde{g}$.

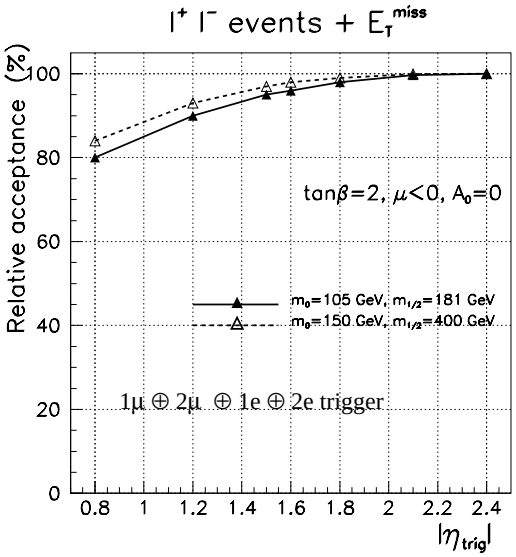

Figure 9: Relative acceptance for $\ell^+\ell^-$ events as a function of muon trigger limit $\eta^{\mu}_{\rm trig}$ with fixed electron trigger limit of $\eta^{e}_{\rm trig}$=2.4.

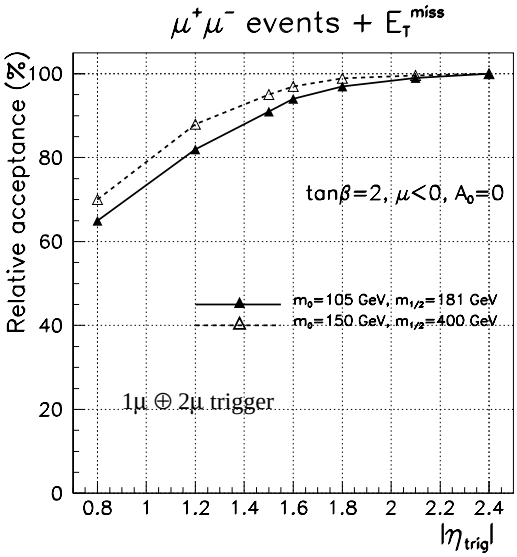

Figure 10: Relative acceptance for $\mu^+\mu^-$ events as a function of muon trigger limit $\eta^{\mu}_{\rm trig}$.

4.3 Multi-lepton final states

In some specific SUSY scenarios the leptonic decays of $\tilde{\chi}^0_2$ can lead to a spectacular sharp edge in the $\ell^+\ell^-$ mass spectrum as already mentioned. Here we discuss the acceptance for muons from $\tilde{\chi}^{\pm}_1/\tilde{\chi}^0_2$ cascade decays via sleptons as in this case they are relatively soft and broader in rapidity when compared to the direct decays. A representative mSUGRA point with $m_0 = 50$ GeV, $m_{1/2} = 125$ GeV, $A_0 = 0$, tan$\beta = 2$ and $\mu < 0$ has been chosen. The masses of relevant sparticles are $M_{\tilde{g}} = 351$ GeV, $M_{\tilde{q}} = 310$ GeV, $M_{\tilde{\mu}_L} = 110$ GeV, $M_{\tilde{\mu}_R} = 78$ GeV, $M_{\tilde{\chi}^0_2} \simeq M_{\tilde{\chi}^{\pm}_1} = 116$ GeV and $M_{\tilde{\chi}^0_1} = 55$ GeV. Two detectable edges are expected from the $\tilde{\chi}^0_2$ decays via left and right sleptons. This point is accessible at the Tevatron with $\sqrt{s} = 2$ TeV, $\int \mathcal{L} = 10^3$ pb^{-1} in a general SUSY particle searches, but not through the observation of edges in the dilepton invariant mass spectrum.

Events were generated by ISAJET with the CTEQ2L structure functions. Inclusive $\tilde{\chi}^0_2$ production and direct $\tilde{\chi}^{\pm}_1\,\tilde{\chi}^0_2$ pair production processes have been considered which can lead to two- and three-muon final states, respectively:

$$\tilde{\chi}^0_2 \longrightarrow \mu\,\tilde{\mu}_L/\tilde{\mu}_R(\rightarrow \mu\tilde{\chi}^0_1) \longrightarrow 2\mu \quad (4.1)$$

$$\tilde{\chi}^{\pm}_1\,\tilde{\chi}^0_2 \longrightarrow \nu\,\tilde{\mu}_L/\tilde{\mu}_R(\rightarrow \mu\tilde{\chi}^0_1)\,\mu\,\tilde{\mu}_L/\tilde{\mu}_R(\rightarrow \mu\tilde{\chi}^0_1) \longrightarrow 3\mu \quad (4.2)$$

Fig. 11 shows the relative acceptance versus $\eta^{\mu}_{\rm trig}$ coverage for these two processes. Reduction of acceptance below $\eta^{\mu}_{\rm trig}\approx$ 1.6-1.8 would result in a significant loss.

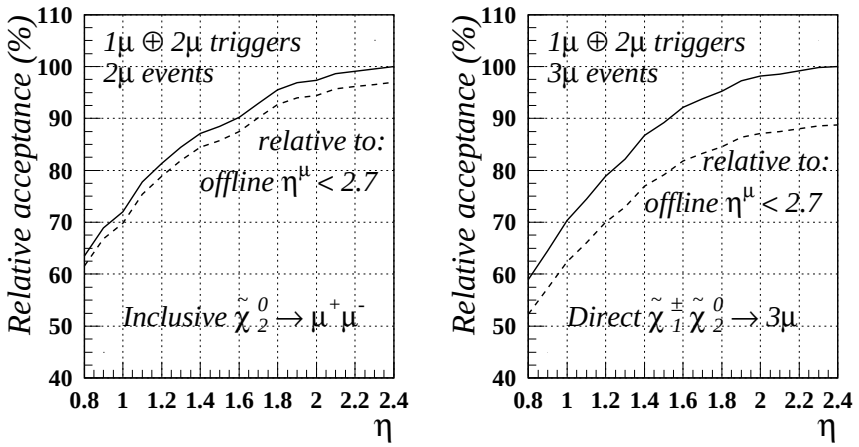

Figure 11: Relative acceptance for SUSY decays as a function of muon trigger limit $\eta^{\mu}_{\rm trig}$ for 1μ and 2μ trigger. $m_0 = 50$ GeV, $m_{1/2} = 125$ GeV.

5 Top quark physics

Top quark production is interesting in itself, as t-quark properties will be among the first topics to be studied at LHC startup: $m_{\rm top}$, branching ratios. Top production is also a way to investigate $H^{\pm}$ production for $m_A \approx m_H \leq$ 120-140 GeV as mentioned in Section 3. Let us discuss sensitivity to muon acceptance.

Events were generated by PYTHIA for a top mass of 175 GeV. The $t\bar{t}$ pair and single top production processes with one or two muons in the final states have been considered:

$$t\bar{t} \longrightarrow W(\rightarrow \mu\nu/\text{jets})\, b(\rightarrow \mu/\text{jet}) \longrightarrow 1\mu/2\mu \quad (5.1)$$
$$Wtb \longrightarrow W(\rightarrow \mu\nu/\text{jets})\, b(\rightarrow \mu/\text{jet}) \longrightarrow 1\mu/2\mu \quad (5.2)$$

The W's and b-quarks were decayed freely. The acceptances have been estimated for low luminosity single and dimuon triggers. Fig. 12 shows the relative acceptance versus $\eta^{\mu}_{\rm trig}$ coverage. In case of two-muon events a logical OR of single and dimuon triggers have been applied.

The possibilities to extract single top production in CMS have not yet been investigated. We might need, for example, tagging of the forward b-jet either by a secondary vertex or via a muon. The current PYTHIA version does not incorporate the exact matrix element for Wtb production, thus our estimates are rather uncertain. Nonetheless it is evident that in case of 1 muon final states, which represents most of top production, the acceptance is directly proportional to $\eta^{\mu}_{\rm trig}$.

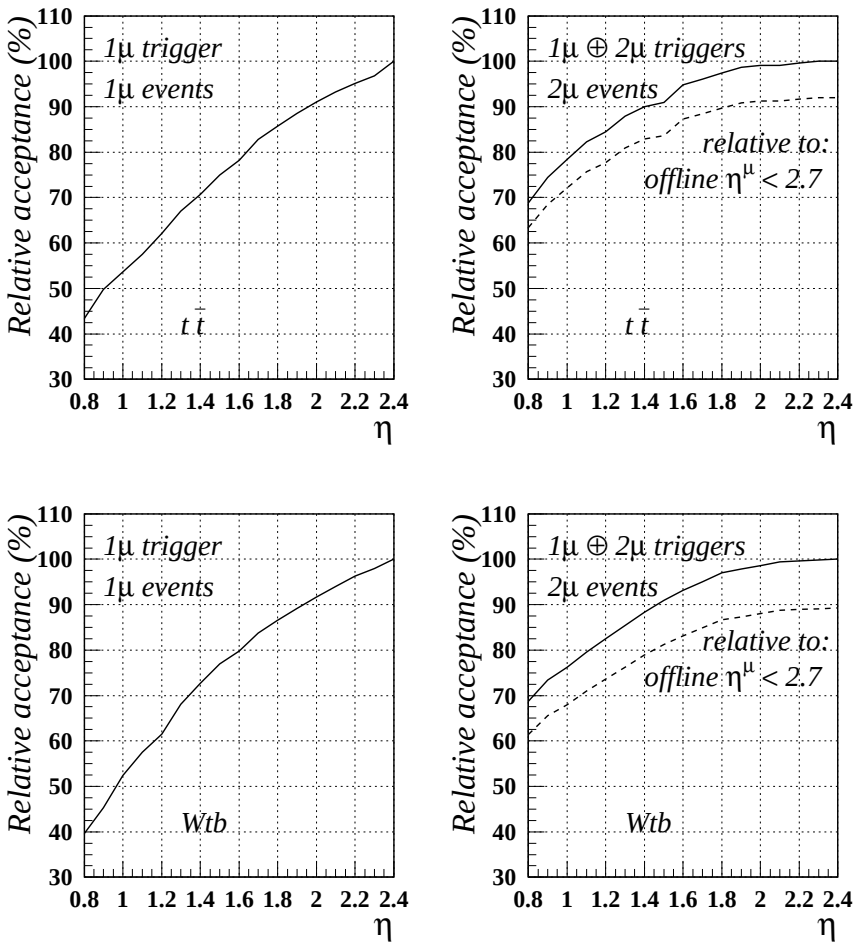

Figure 12: Relative acceptance for top production channels as a function of muon trigger acceptance limit $\eta^{\mu}_{\rm trig}$ for 1μ and 2μ triggers; $m_{\rm top} = 175$ GeV.

6 The *b*-quark physics

The highest losses due to the reduction of trigger acceptance are expected in *b*-physics as decay muons are softer than in channels already discussed, with long flat plateau in rapidity. The following five reactions have been considered, with various numbers of muons in the final state:

$$
\begin{array}{lllll}
b\bar{b} & \longrightarrow & B_d^0(\rightarrow \pi^+\pi^-) + \mu + ... & \longrightarrow 1\mu & (6.1)\\
 & \longrightarrow & B_s^0(\rightarrow \mu^+\mu^-) + ... & \longrightarrow 2\mu & (6.2)\\
 & \longrightarrow & \mu^+\mu^- + ... & \longrightarrow 2\mu & (6.3)\\
 & \longrightarrow & J/\psi(\rightarrow \mu^+\mu^-) + ... & \longrightarrow 2\mu & (6.4)\\
 & \longrightarrow & B_d^0(\rightarrow J/\psi K_S^0) + \mu + ... & \longrightarrow 3\mu & (6.5)
\end{array}
$$

The results obtained for reaction (6.1) can be extended for reaction (6.1') having very similar kinematics:

$$b\bar{b} \longrightarrow B_s^0(\rightarrow D_s^{\pm}\pi^{\mp} \rightarrow \pi^+\pi^- K^+K^-) + \mu + ... \longrightarrow 1\mu \quad (6.1')$$

Events were generated with PYTHIA 5.7, the CTEQ2L structure functions. Only the gg-fusion mechanism of $b\bar{b}$ production has been considered (g-splitting yields similar p_t and rapidity spectra). The acceptances have been estimated for the low luminosity trigger thresholds. Fig. 13 shows the relative acceptance versus the $\eta^{\mu}_{\rm trig}$ coverage of the muon trigger. The dimuon trigger is applied for the channels with ≥ 2 muons in the final states.

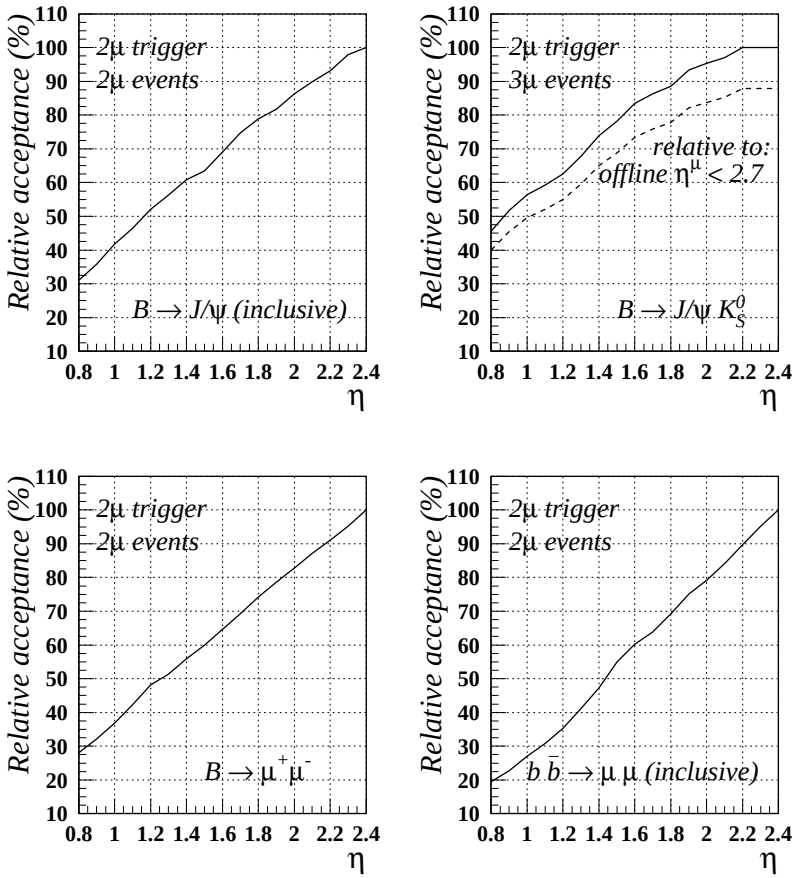

Figure 13: Relative acceptance for *b*-physics channels as a function of muon trigger limit $\eta^{\mu}_{\rm trig}$ for 2μ trigger.

Fig. 14 shows the relative acceptance versus $\eta^{\mu}_{\rm trig}$, but now for single and dimuon triggers combined in a logical OR for 2μ and 3μ events. The two-muon channels are most affected by the reduction of $\eta^{\mu}_{\rm trig}$. This is because muons from *b*-decays are rather soft and they rarely cross the single muon trigger threshold of 7 GeV.

For the ultimate *b*-physics performance estimates in CMS, at the first-level dimuon trigger η dependent p_t thresholds have been considered up to now [9], with $p_t > 4.5$, 3.6 and 2.6 GeV for $\eta^{\mu}_{\rm trig} < 1.5$, 2.0 and 2.4, respectively. In this case the relative loss in acceptance due to the trigger descoping is much more significant. In reaction (6.4) for example, trigger limit at $|\eta| < 1.6$ retains only about 20 % of dimuon events [10] compared to 70 % retained in current analysis with a simplified dimuon trigger including no η dependent thresholds.

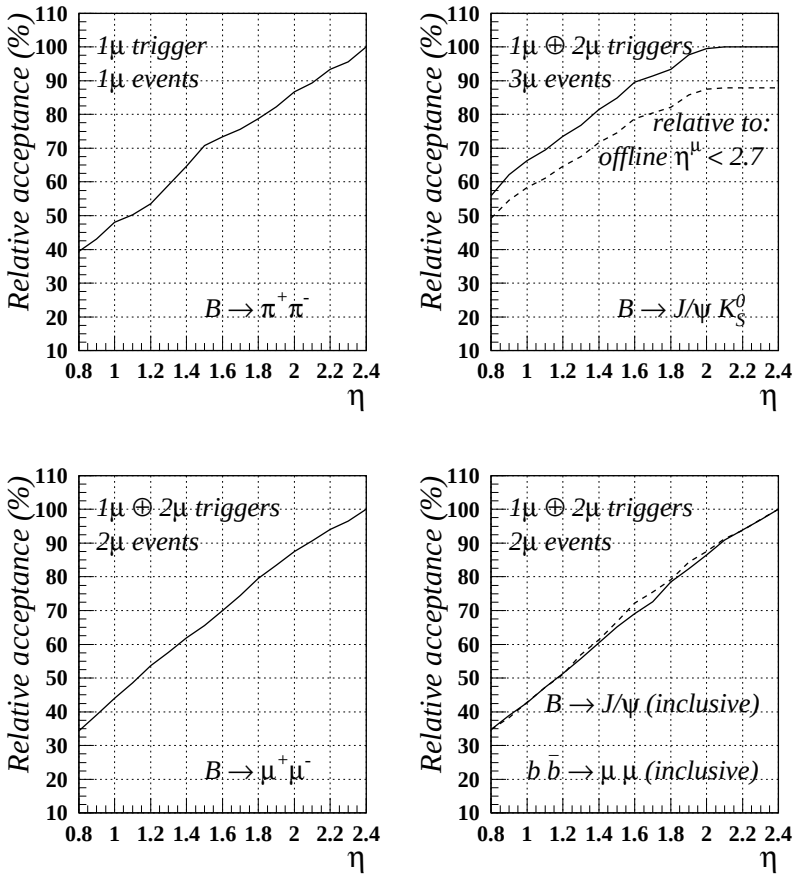

Figure 14: Relative acceptance for b-physics channels as a function of muon trigger limit $\eta^{\mu}_{\rm trig}$ for 1μ and 2μ trigger.

7 Heavy ion physics — J/ψ and Υ detection

There are strong differences in the detection of J/ψ and Υ between the barrel and the endcaps in CMS. In the barrel, each muon must have a high enough p_t to reach the muon chambers, $p_t > 3.5$ GeV. This is not the case for the endcaps. The effect is most dramatic for the J/ψ which is strongly suppressed in the barrel. Practically no J/ψ with $p_t < 6$ GeV will be detected in the barrel. If we want to go to lower p_t ψ production we must be able to detect and measure the dimuons in the endcaps. For the Υ the main consequence is a limitation in statistics, which is not negligible. In the barrel alone we expect 30000 Υ(1S) per month of running time with Pb beams at nominal luminosity. The situation is more favourable for lighter ion beams for which the luminosities are much higher. But for Pb beams, this statistics is not really comfortable, as we must study the collisions as a function of their centrality deduced from the ECAL information. Further on, we must do (M, p_t) correlations. Extending the detection to the full rapidity range ($|\eta| < 2.4$) will double the number of measured Υ(1S), assuming the same dimuon reconstruction efficiency in endcaps and in barrel, which has not been proved yet. This extension also reinforces the competitiveness of CMS vs ALICE for this type of studies. The situation is summarized in Table 4. The numbers are slightly different from those quoted above. The numbers in the table are calculated with old reconstruction efficiency coefficients. In a minimum bias Pb-Pb collision the reconstruction efficiency was about 68 % whilst it is now estimated to be 88 % in the barrel, for a V3 tracker without descoping.

Table 4: Acceptances, expected statistics and signal/background ratios in 1 month with Pb beams, in full CMS acceptance and in barrel only.

full CMS	J/ψ	Υ	Υ'
acceptance	7%	35%	
statistics	580000	55000	20000
S/B	0.17	0.8	

barrel region	J/ψ	Υ	Υ'
acceptance	0.07%	9%	
statistics	31000	23000	8300
S/B	1.8	1.6	

8 Summary and conclusions

The studies presented in previous sections are summarised in Table 5 and Figures 15 and 16. It can be seen that reducing the trigger coverage down to $\eta^{\mu}_{\rm trig}$=2.1 does not reduce the physics acceptance for any of the channels investigated by more than 10%. Limiting the trigger to $\eta^{\mu}_{\rm trig}$=1.6 separates the channels under study in three groups. SM and SUSY Higgs searches in $4\ell^{\pm}$, $h, H, A \to \mu\mu$ and squark/gluino searches are not affected by more than 10%. The $h, H, A \to \tau\tau$ and top physics (including $H^{\pm} \to \tau\nu$) acceptance is reduced by 20-25%. Most of the b-physics channels suffer a loss of about 30%. Further decrease of the trigger coverage would have a dramatic effect on all the physics channels investigated.

Table 5: Relative acceptance as a function of muon trigger limit $\eta^{\mu}_{\rm trig}$ for 1μ and 2μ triggers, normalized to $\eta^{\mu}_{\rm trig}$=2.4. The numbers given for A^0 are also valid for H^0 and h^0.

			$\eta^{\mu}_{\rm trig}$	2.1	1.6	1.2	0.8
$H \to ZZ^{(*)} \to 4\mu$				100	96	88	60
	m_A	$\tan\beta$					
$A^0 \to \tau\tau \to 1\mu$+jet	140	20		94	76	59	41
$A^0 \to \tau\tau \to 1\mu + 1e$	140	20		94	76	59	41
$gg \to A^0 \to 2\mu$	120	30		97	89	78	59
$gg \to A^0 b\bar{b} \to 2\mu$	120	30		100	97	90	78
	m_0	$m_{1/2}$					
SUSY$_1 \to 1\mu$	80	180		97	90	80	67
SUSY$_2 \to 1\mu$	500	150		98	92	82	67
SUSY$_3 \to 1\mu$	200	150		99	96	90	81
SUSY$_4 \to 2\mu$	105	181		98	94	82	65
SUSY$_5 \to 2\mu$	150	400		99	96	88	70
SUSY$_6 \to 2\mu$	50	125		98	90	81	64
SUSY$_6 \to 3\mu$	50	125		98	92	78	59
$t\bar{t} \to 1\mu$				93	78	62	44
$t\bar{t} \to 1\mu + H^{\pm} \to \tau$-jet				93	78	62	44
$Wtb \to 1\mu$				93	80	62	40
$t\bar{t} \to 2\mu$				99	95	84	69
$Wtb \to 1\mu$				99	93	82	69
$B \to J/\psi K^0_s \to 3\mu$				100	90	73	56
$B \to J/\psi \to 2\mu$ (incl.)				91	69	52	35
$B \to 2\mu$				91	70	53	35
$b\bar{b} \to 2\mu$ (incl.)				91	72	52	35
$B \to \pi\pi + 1\mu$				89	73	53	39
$B \to \pi\pi\, KK + 1\mu$ (oscillations)				89	73	53	39

Clearly, this is not an exclusive list of channels but it is illustrative enough of the potential loss. A channel such as $H \to WW \to \mu\nu\,\mu\nu$ or $\mu\nu\, e\nu$ (for $m_H \sim$130-200 GeV) could be affected — qualitatively — as $A \to \tau\tau$; $h \to \gamma\gamma$ from Wh with $W \to \mu\nu$ should be affected comparably to $t\bar{t}$; $A \to Zh \to \mu\mu\, b\bar{b}$ comparably to $b\bar{b}A \to \mu\mu$, etc.

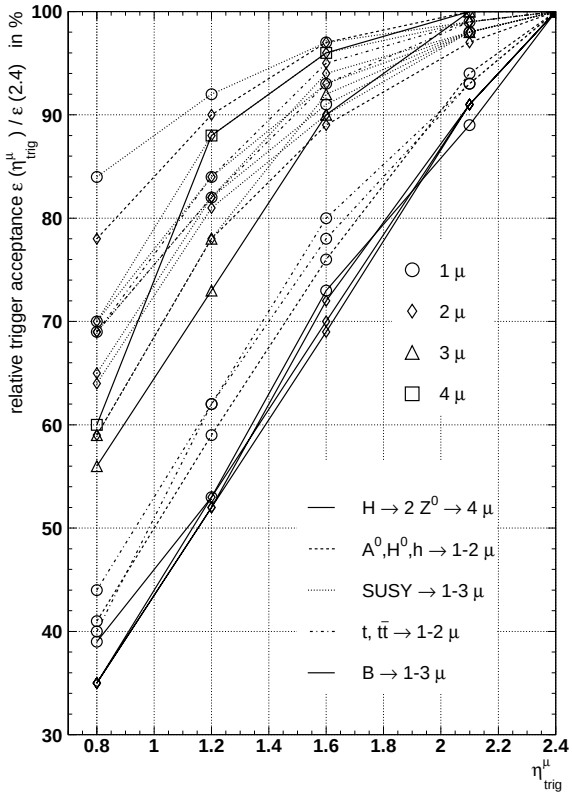

Figure 15: Relative acceptance as a function of muon trigger limit $\eta^{\mu}_{\mathrm{trig}}$ for 1μ and 2μ triggers.

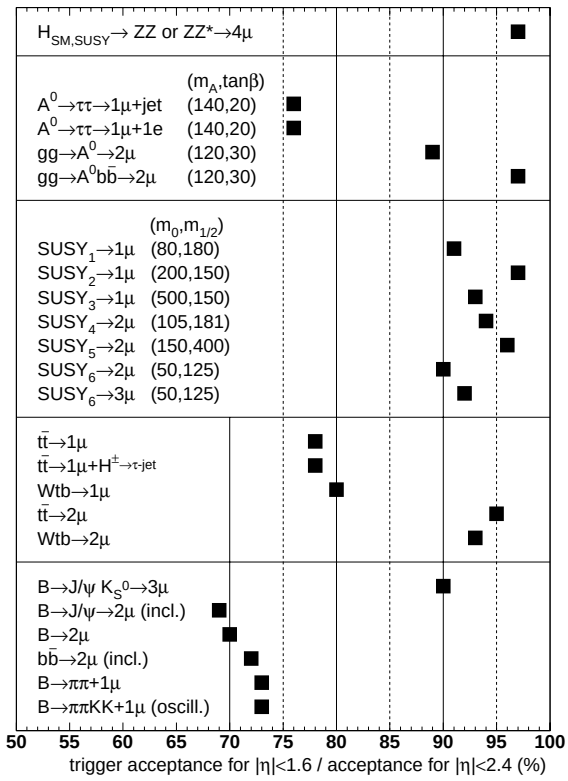

Figure 16: Relative acceptance for the muon trigger limit $\eta^{\mu}_{\mathrm{trig}}$=1.6, for 1μ and 2μ triggers. The numbers given for A^0 are also valid for H^0 and h^0.

Appendix: Trigger thresholds

Another tool for controlling the trigger rate is the p_t threshold of muon triggers and transverse energy threshold of calorimeter triggers. In the case of multi-object triggers (like e.g. $e\mu$ trigger) the optimal threshold can be different for different combinations of objects.

Proposed sets of thresholds for triggers involving a muon are given in Table 6 for three different limits on Second Level Trigger (LV2) input rates. The threshold denoted by "2-4" means, the minimal possible p_t threshold, which is approximately 4 GeV in the barrel and 2 GeV in the endcaps. The safety factor of 3 is required, i.e. the total output rate of LV1 should be 3 times lower than the LV2 input limit. It was assumed that the available bandwidth is equally divided between purely calorimetric triggers and triggers involving at least one muon.

Table 6: Trigger rates for selected thresholds at $\mathcal{L} = 10^{33}\mathrm{cm}^{-2}\mathrm{s}^{-1}$.

LV2 input rate = 100 kHz				
trigger type	thresholds (GeV)		rate (kHz)	
			individual	cumulative
μ	7		7.0	7.0
$\mu\,\mu$	2-4		0.5	7.3
$\mu\,e$	2-4	7	2.4	9.2
$\mu\,e_b$	2-4	4	5.2	12.8
μ j	2-4	10	4.2	14.4
$\mu\,E_t^{\mathrm{miss}}$	2-4	40	0.2	14.4
$\mu\,\Sigma E_t$	2-4	100	0.7	14.4

LV2 input rate = 75 kHz				
trigger type	thresholds (GeV)		rate (kHz)	
			individual	cumulative
μ	7		7.0	7.0
$\mu\,\mu$	2-4		0.5	7.3
$\mu\,e$	2-4	7	2.4	9.2
$\mu\,e_b$	2-4	4.5	3.3	11.1
μ j	2-4	15	2.0	11.9
$\mu\,E_t^{\mathrm{miss}}$	2-4	40	0.2	11.9
$\mu\,\Sigma E_t$	2-4	100	0.7	11.9

LV2 input rate = 50 kHz				
trigger type	thresholds (GeV)		rate (kHz)	
			individual	cumulative
μ	8		4.2	4.2
$\mu\,\mu$	2-4		0.5	4.6
$\mu\,e$	2-4	8	1.3	5.6
$\mu\,e_b$	2-4	5	2.6	7.0
μ j	2-4	15	2.0	8.0
$\mu\,E_t^{\mathrm{miss}}$	2-4	40	0.2	8.0
$\mu\,\Sigma E_t$	2-4	100	0.7	8.0

References

[1] *PYTHIA 5.7 and JETSET 7.4 Physics and Manual*, T.Sjöstrand, **CERN-TH.7112/93**, **LU TP 95-20** T.Sjöstrand, *Computer Physics Commun.* **82** (1994) 74.

[2] H. Baer, C.-H. Chen, F. Paige and X. Tata, Phys.Rev. **D53** (1996) 6241.

[3] S. Abdullin, **CMS TN/96-095**.

[4] S. Abdullin, *et al.*, **CMS NOTE 1998/006**.

[5] F. Paige and S. Protopopescu, in *Supercollider Physics*, p. 41, ed. D. Soper (World Scientific, 1986); H. Baer, F. Paige, S. Protopopescu and X. Tata, in *Proceedings of the Workshop on Physics at Current Accelerators and Supercolliders*, ed. J. Hewett, A. White and D. Zeppenfeld (Argonne National Laboratory, 1993).

[6] S. Abdullin, A. Khanov and N. Stepanov, **CMS TN/94-180** (see also /afs/cern.ch/user/a/abdullin/public/cmsjet/4.4/).

[7] D. Denegri, W. Majerotto, and L. Rurua, **CMS NOTE 1997/094**, **hep-ph/9711357**.

[8] *The Compact Muon Solenoid – Letter of Intent*, **CERN/LHCC 92-3**, October 1992.

[9] *The Compact Muon Solenoid – Technical Proposal*, **CERN/LHCC 94-38**, December 1994.

[10] A. Kharchilava, P. Pralavorio, **CMS TN/96-117**.